GPS Solutions (2023) 27:84
https://doi.org/10.1007/s10291-023-01398-5

GPS TOOLBOX

Open-source software for multi-GNSS inter-frequency clock bias estimation

Xingxing Li[1] · Hongjie Zheng[1] · Xin Li[1] · Yongqiang Yuan[1] · Jiaqi Wu[1] · Xinjuan Han[1]

Received: 29 September 2021 / Accepted: 11 January 2023 / Published online: 10 March 2023

Abstract

As one of the key issues in multi-frequency Global Navigation Satellite System (GNSS) applications, the inter-frequency clock bias (IFCB) has been well studied in recent years. However, the lack of publicly available IFCB products prevents users from taking full advantages of multi-frequency GNSS observations. An open-source software called GREAT-IFCB, which is derived from the GNSS + REsearch, Application and Teaching (GREAT) software platform at Wuhan University, is designed and developed to provide multi-GNSS IFCB products for multi-frequency users. Based on the geometry-free and ionospheric-free combinations of the multi-frequency observations, GREAT-IFCB can generate IFCB products for GPS, Galileo and BDS satellites. Multi-frequency observations from day of year 001 to 007 of 2021 were selected to estimate the multi-GNSS IFCB products for demonstrating the performance of GREAT-IFCB. After applying the IFCB corrections, the averaged standard deviation (STD) of estimated extra-wide-lane (EWL) uncalibrated phase delay (UPD) for GPS satellites is improved by 68.4% from 0.076 cycles to 0.024 cycles, and the positioning accuracy of triple-frequency PPP is improved by 30.3%, 32.9% and 31.6% in the east, north and up components, respectively.

Keywords GREAT-IFCB · Open-source software · Inter-frequency clock bias · Multi-GNSS · Multi-frequency

Introduction

As one of the representative positioning technologies, the traditional precise point positioning (PPP) takes a long time to initialize (Malys and Jensen 1990; Zumberge et al. 1997). Over the past decade, GNSS has rapidly developed with abundant networks, modern constellations and multi-frequency observations. Meanwhile, several new mathematic models were researched to improve the positioning performance of PPP, such as the rapid ambiguity resolution (AR) with uncalibrated phase delay (UPD) products (Gu et al. 2015; Li et al. 2019, 2020), the precise atmospheric corrections augmentation (Li et al. 2021b), and the fusion of multi-GNSS and multi-frequency observations (Moreno et al. 2014; Guo et al. 2016b; Deo and El-Mowafy 2018; Li et al. 2018; Liu et al. 2019).

Taking full advantage of multi-frequency GNSS observations, the positioning accuracy and convergence time of PPP can be obviously improved. The performance of GPS triple-frequency PPP has been investigated by Deo and El-Mowafy (2018), and triple-frequency PPP AR was realized by Geng and Bock (2013) based on simulated GPS triple-frequency observations. Later, more experiments about triple-frequency PPP based on BDS and Galileo observations have been conducted (Guo et al. 2016a; Li et al. 2018, 2019). Furthermore, with the availability of five frequency observations of Galileo (Wang et al. 2018), five-frequency PPP AR was conducted by Li et al. (2020) to improve the performance of PPP further.

However, the satellite clock products provided by the International GNSS Service (IGS) are usually derived from the ionospheric-free (IF) combination of two specific

The GPS Tool Box is a column dedicated to highlighting algorithms and source code utilized by GPS engineers and scientists. If you have an interesting program or software package you would like to share with our readers, please pass it along; e-mail it to us at gpstoolbox@ngs.noaa.gov. To comment on any of the source code discussed here, or to download source code, visit our website at http://www.ngs.noaa.gov/gps-toolbox. This column is edited by Stephen Hilla, National Geodetic Survey, NOAA, Silver Spring, Maryland, and Mike Craymer, Geodetic Survey Division, Natural Resources Canada, Ottawa, Ontario, Canada.

✉ Xin Li
lixinsgg@whu.edu.cn

[1] School of Geodesy and Geomatics, Wuhan University, 129 Luoyu Road, Wuhan 430079, China

frequencies (Hauschild and Montenbruck 2009; Bock et al. 2009; Ge et al. 2012) and are not appropriate for multi-frequency PPP processing. This can be attributed to the frequency-specific and time-varying biases included in carrier phase observations. Montenbruck et al. (2012) first found the time-varying biases on GPS carrier phase observations based on Geometry-Free and Ionospheic-Free (GFIF) combinations. The biases were defined as the inter-frequency clock bias (IFCB), which was confirmed to be the same as the difference between the satellite clock products based on L1/L2 and L1/L5 IF combined observations (Montenbruck et al. 2012). The amplitude of IFCB variation on GPS can reach to 10 cm level (Montenbruck et al. 2012), while BDS and Galileo satellites exhibit the smaller variation (Montenbruck et al. 2013; Cai et al. 2016; Zhao et al. 2016; Pan et al. 2017). Therefore, the IFCB issues hinder the application of multi-frequency observations, especially on GPS.

On this basis, Li et al. (2012) proposed an epoch-differenced (ED) approach for IFCB estimation. Due to the elimination of the phase ambiguities, the ED approach can generate IFCB products efficiently, which is quite suitable in real-time applications. Beyond that, IFCB products can also be directly derived from the two sets of satellite clock products generated in triple-frequency precise clock estimation (PCE) (Guo and Geng 2018). Meanwhile, several IFCB estimation method based on multi-frequency UC observations has been proposed. Fan et al. (2019) used UC multi-frequency model to estimate IFCB for GPS satellites, and Pan et al. (2019) established a unified model for IFCB estimation, which can be adapted in multi-frequency PPP processing with UC and IF observations.

There is no doubt that the IFCB estimation is important to realize GNSS applications with multi-frequency observations, such as multi-frequency PPP and multi-frequency UPD estimation. Yet, there are no IFCB products or open-source software about IFCB estimation for users. For this reason, we developed an open-source software named GREAT-IFCB, which can freely generate multi-GNSS IFCB products based on multi-frequency observations. The software is released under the terms of the GNU General Public License (version 3).

After this introduction, the main structure of GREAT-IFCB is presented. Subsequently, the characteristic of multi-GNSS IFCB products generated by GREAT-IFCB is shown. With the estimated IFCB products, the results of estimated EWL UPDs and multi-frequency PPP are also displayed. Finally, the conclusions are provided.

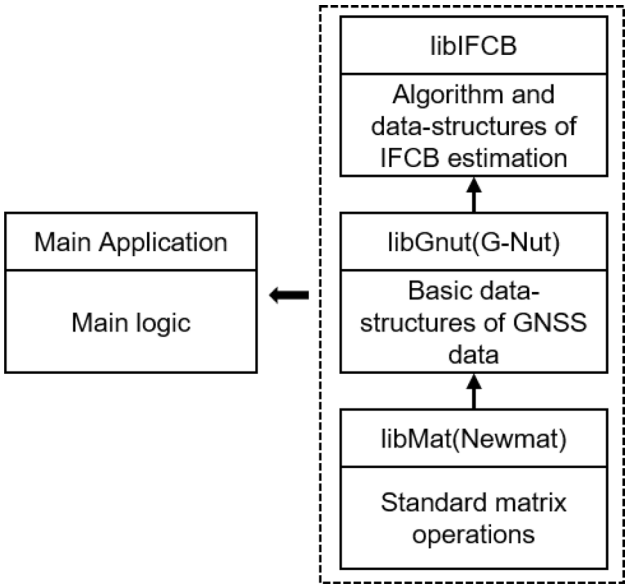

Fig. 1 Relationship of GREAT-IFCB composition

Overview of GREAT-IFCB

Similar to GREAT-UPD (Li et al. 2021a), GREAT-IFCB is also an important module of the GREAT (GNSS + REsearch, Application and Teaching) software platform. GREAT is designed and developed at Wuhan University for scientific and engineering application and teaching in geodesy and navigation fields. More information about the GREAT software can be accessed on the website https://igmas.users.sgg.whu.edu.cn/software.

GREAT-IFCB is designed according to the principles of modularity and extensibility. We chose the object-oriented programming language C + + to develop source code for its strong abstraction, high efficiency and cross-platform characteristic. Therefore, GREAT-IFCB supports several common operating systems, i.e., Windows, Linux, and Macintosh. Furthermore, for building and packaging the software more conveniently, building tool CMake is employed on GREAT-IFCB.

GREAT-IFCB is released under the terms of GNU General Public License (version 3). The source code and executable programs of GREAT-IFCB can be accessed on the website https://geodesy.noaa.gov/gps-toolbox. To facilitate the use of GREAT-IFCB, examples and a user manual are also involved in the software package.

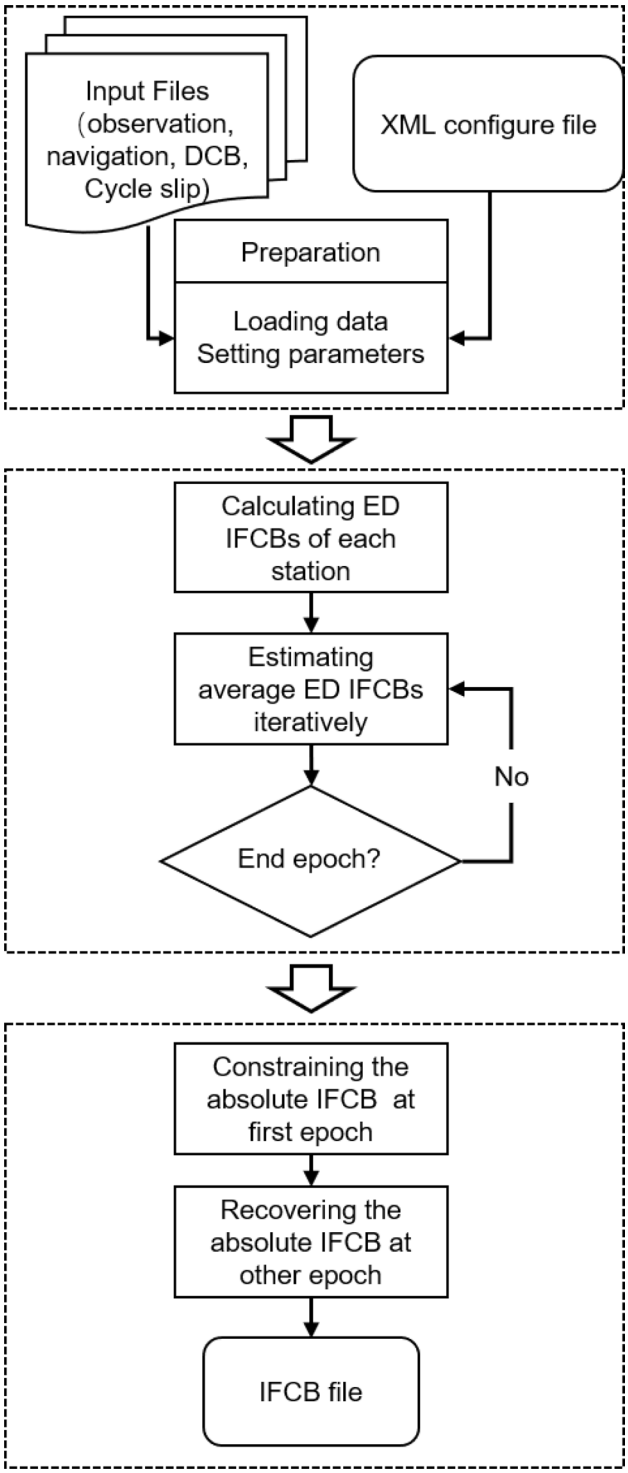

Fig. 2 Flowchart of IFCB estimation based on GREAT-IFCB

Structure of GREAT-IFCB

GREAT-IFCB can be divided into the main application part and the supporting library part. The supporting library part includes libIFCB, libMat and libGnut. Figure 1 shows the relationship between these components. The libIFCB library is the main part of the supporting library part, which realizes the algorithm and data structures about the IFCB estimation. In addition, libMat and libGnut are the auxiliary libraries, wherein the libMat library offers the standard matrix operations, and it comes from the newmat matrix library (an open-source C++matrix library); the libGnut library offers the basic data structures of GNSS data and it derives from the G-Nut (an open-source C++GNSS software, Vaclavovic et al. 2013).

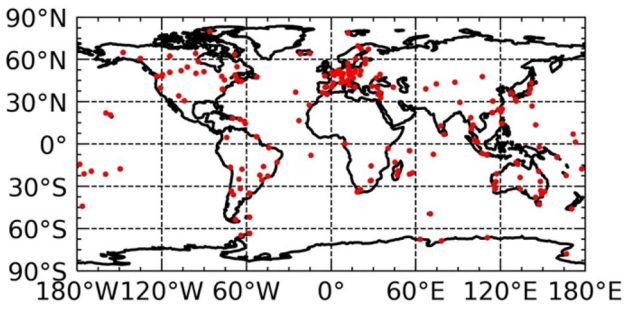

Fig. 3 Distribution of the stations used for IFCB estimation

IFCB processing procedure

Figure 2 shows the flowchart of IFCB estimation based on GREAT-IFCB. The processing procedure of IFCB estimation mainly includes three steps: preparation, estimation and production.

The preparation part loads the input data and sets parameters according to the configuration file in Extensible Markup Language (XML) format. The input files for IFCB estimation include observation files, navigation files, DCB files, and multi-frequency cycle slips files. The observation frequency list can be specified in the configure file, and it should be consistent to the cycle slips files. The cycle slips file is a custom file and it contains the information about ambiguity cycle slip. The user manual includes details and descriptions of these input files and setting parameters.

The ED IFCB values are calculated epoch by epoch in the estimation part. First, the GFIF combination values of each station will be calculated. Then, the ED IFCB values for each station can be obtained from GFIF combination data and cycle slips data. Finally, average ED IFCB values can be estimated epoch by epoch according to (8). The estimation will be conducted iteratively for improving the robustness, and the outlier greater than three times of standard deviations (STD) will be removed in each iteration. If the number of outliers is zero or the number of iterations is greater than 10, the estimation will be terminated.

Table 1 Frequency list used for IFCB estimation

System	Frequency Bands
GPS	L1, L2, L5
Galileo	E1, E5a, E5b
BDS-2	B1I, B2I, B3I
BDS-3	B1I, B2a, B3I
	B1C, B2a, B3I

The production part will add a constraint and calculate the undifferenced IFCB values of all epochs. The zero-mean constraint will be added according to (10). Therefore, the undifferenced IFCB values of each satellite at the reference epoch are determined. Based on these initial values and (9), the undifferenced IFCB values of other epochs can be obtained by the cumulative method.

Performances of GREAT-IFCB

In this section, observations of 250 Multi-GNSS Experiment (MGEX, Montenbruck et al. 2017) stations (shown in Fig. 3) from day of year (DOY) 001 to 007 of 2021 are utilized to validate IFCBs estimated by GREAT-IFCB software. The characteristic of IFCB products is displayed, and the results calculated by the precise clock estimation method are also given as a comparison. Moreover, based on the estimated IFCB products, the UPD estimated results and triple-frequency PPP results are analyzed to illustrate the benefits of the IFCB products.

Characteristic of the estimated IFCB products

In the process of IFCB estimation, the DCB products of the Institute of Geodesy and Geophysics (IGG) are used and the frequency list is given in Table 1. The estimated IFCB series from DOY 001 to 007 of 2021 for GPS and Galileo satellites are displayed in Fig. 4 and Fig. 5, respectively, which include all satellites providing multi-frequency observations. Figure 4 shows the results of GPS Block IIF and the new Block III satellites (G04, G14, G18 and G23). The peak-to-peak amplitude is about 10 cm for the GPS Block IIF satellites but less than 2 cm for the GPS III satellites, indicating that PIFCB errors barely influence the L5 carrier phase observations of GPS III satellites, which has also been confirmed by Thoelert et al. (2019). Meanwhile, from Fig. 5, it can be found that the PIFCB values of all Galileo satellites exhibit a variation of less than 2 cm.

The root-mean-square (RMS) statistics of the estimated IFCBs for GPS and Galileo satellites are shown in the top

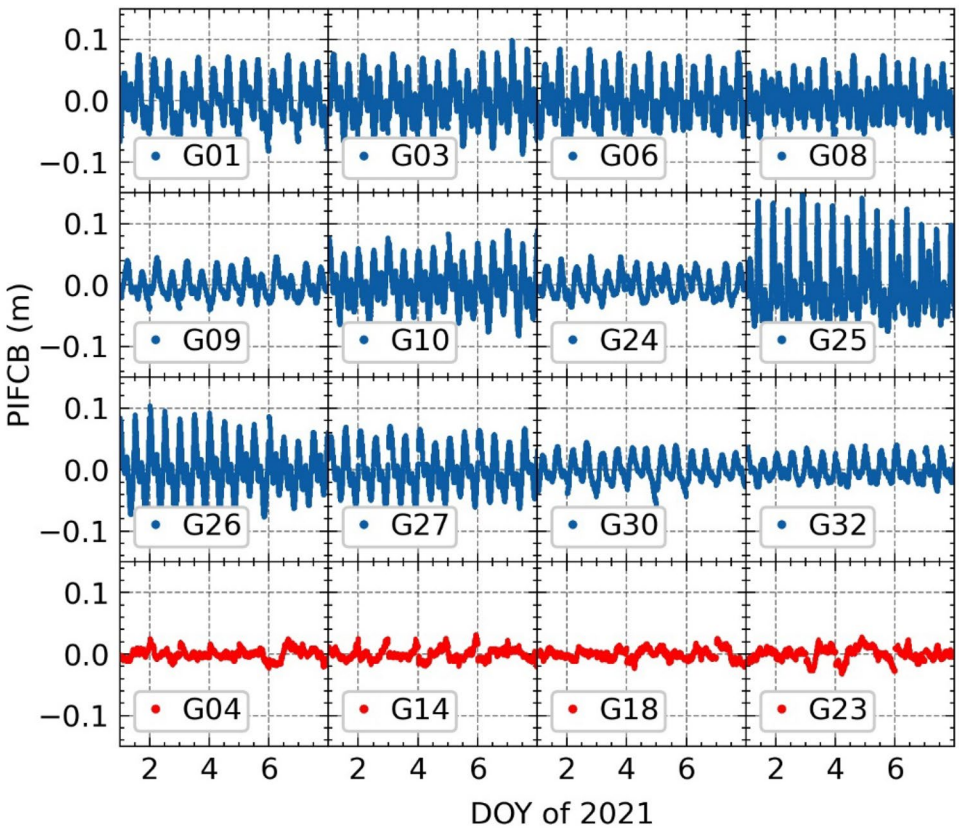

Fig. 4 IFCB estimation results for GPS satellites from DOY 001 to 007 of 2021. The blue dots denote GPS Block IIF satellites and the red dots denote GPS III satellites

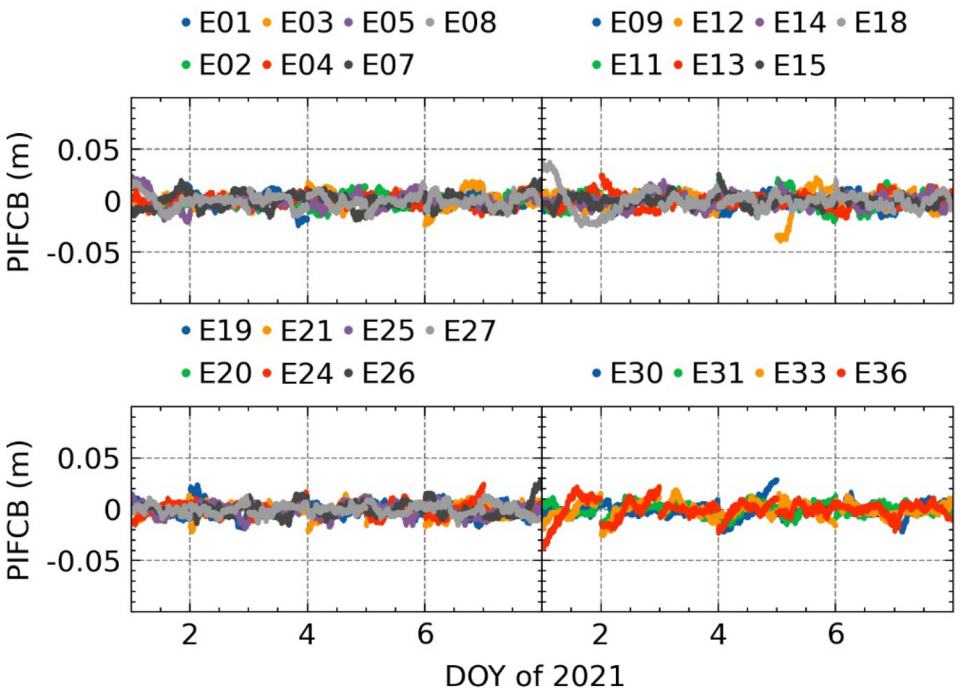

Fig. 5 IFCB estimation results for Galileo satellites from DOY 001 to 007 of 2021

and bottom panels of Fig. 6, respectively. The RMS values of GPS III and Galileo satellites are smaller than 1 cm, which means that PIFCB errors of GPS III and Galileo satellites can both be ignored.

Figure 7 shows the IFCB estimation results of BDS satellites from DOY 001 to 007 of 2021, and Fig. 8 shows the RMS statistics of the estimated IFCBs of BDS satellites. In Figs. 7 and 8, the results of BDS-2 satellites with B1I/B2I/B3I, BDS-3 satellites with B1C/B2a/B3I and BDS-3 satellites with B1I/B2a/B3I are depicted from top to bottom, respectively. For most BDS satellites, it can be found that the amplitude of PIFCB values is about 3–4 cm and the RMS values are smaller than 2 cm. However, the satellites starting from C40 show larger RMS values than other BDS satellites, which can be attributed to the fewer IGS tracking stations of these new BDS-3 satellites. Due to the fewer observations, the estimated PIFCB values will contain the larger unmodeled bias noise. With the increase in the number of new BDS-3 satellites observations, IFCB estimation results of new BDS-3 satellites will be comparable with other BDS-3 satellites. Besides that, from the middle and bottom panels of Figs. 7 and 8, the BDS-3 IFCB estimation results based on B1C/B2a/B3I and B1I/B2a/B3I frequency observations are almost comparable.

At the same time, we also calculate the GPS IFCB products based on the PCE method for comparison. The same observations on DOY 007 of 2021 are used in the PCE processing. The IFCB results can be obtained by differencing the GPS satellite clock offsets calculated with L1/L2 and L1/L5 observations. Figure 9 shows the difference of IFCB results between GFIF method and PCE method. The RMS values of the difference of each satellite are computed and given in each subfigure. It can be found that the RMS values of all GPS satellites are smaller than 2 cm and most of them are smaller than 1 cm, indicating the good consistency between the two IFCB estimation methods.

Benefits of the estimated IFCB products on multi-frequency data processing

To further verify the reliability of our IFCB products, we investigate the benefits of the estimated IFCB products on multi-frequency data processing. The marginal IFCB variations could be neglected for the Galileo satellites (Cai et al. 2016) and global BDS satellites (Pan et al. 2017), and the experiments therefore mainly focus on the GPS constellation. The results of estimated EWL UPDs are first shown, and the performance of GPS-only triple-frequency PPP with UC model is then described.

Figure 10 shows the estimated EWL UPDs for GPS satellites on DOY 001 of 2021. The estimated EWL UPDs without and with the estimated IFCB products are shown in the top and bottom panels of Fig. 10, respectively. Here, EWL UPDs are estimated epoch by epoch, and G01 is chosen as the reference satellite. Long-term fluctuations with a peak-to-peak amplitude about 0.2–0.4 cycles can be observed in estimated EWL UPDs, if the IFCB corrections are not applied. After correcting the PIFCB errors with the estimated IFCB products, the estimated EWL UPD series

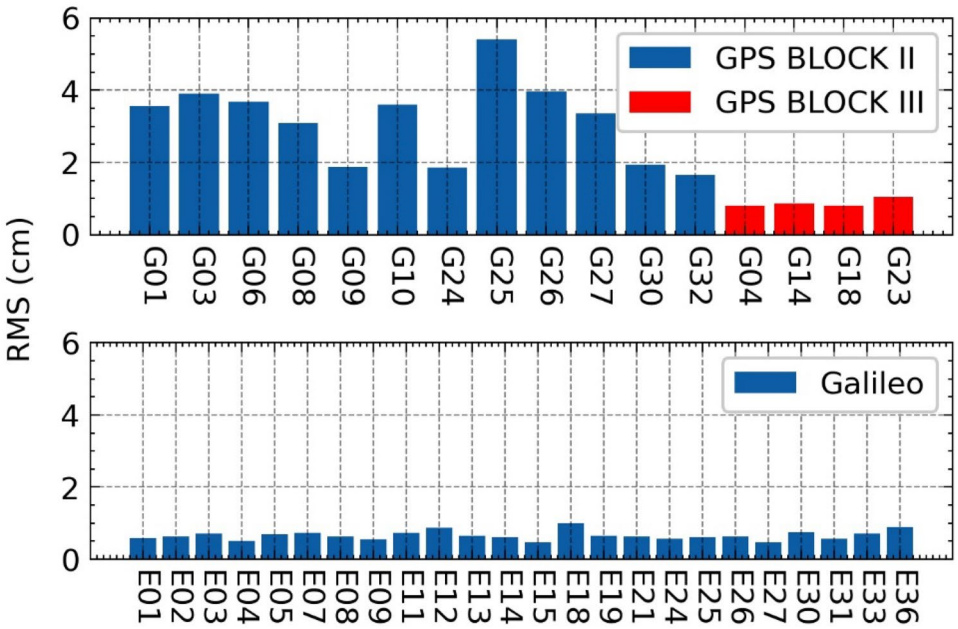

Fig. 6 RMS statistics of the estimated IFCBs for GPS (top) and Galileo (bottom) satellites

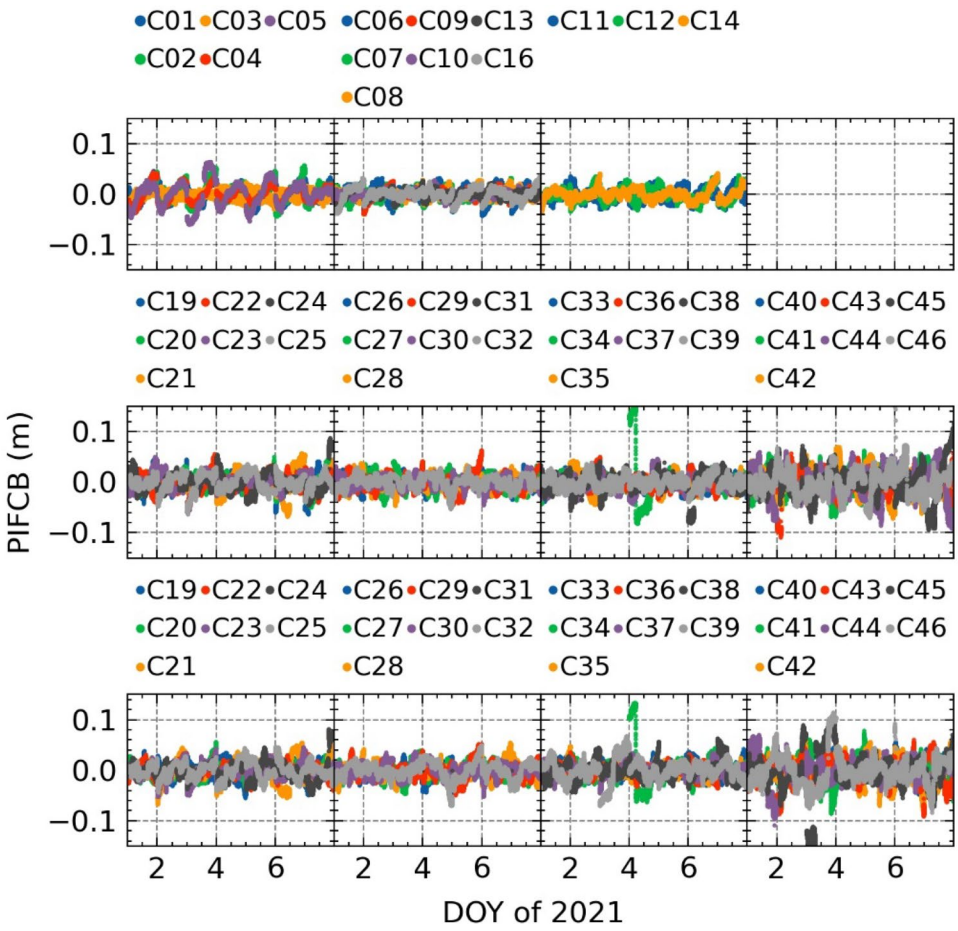

Fig. 7 IFCB estimation results for BDS-2 (top: B1I/B2I/B3I) and BDS-3 (middle: B1C/B2a/B3I; bottom: B1I/B2a/B3I) satellites from DOY 001 to 007 of 2021

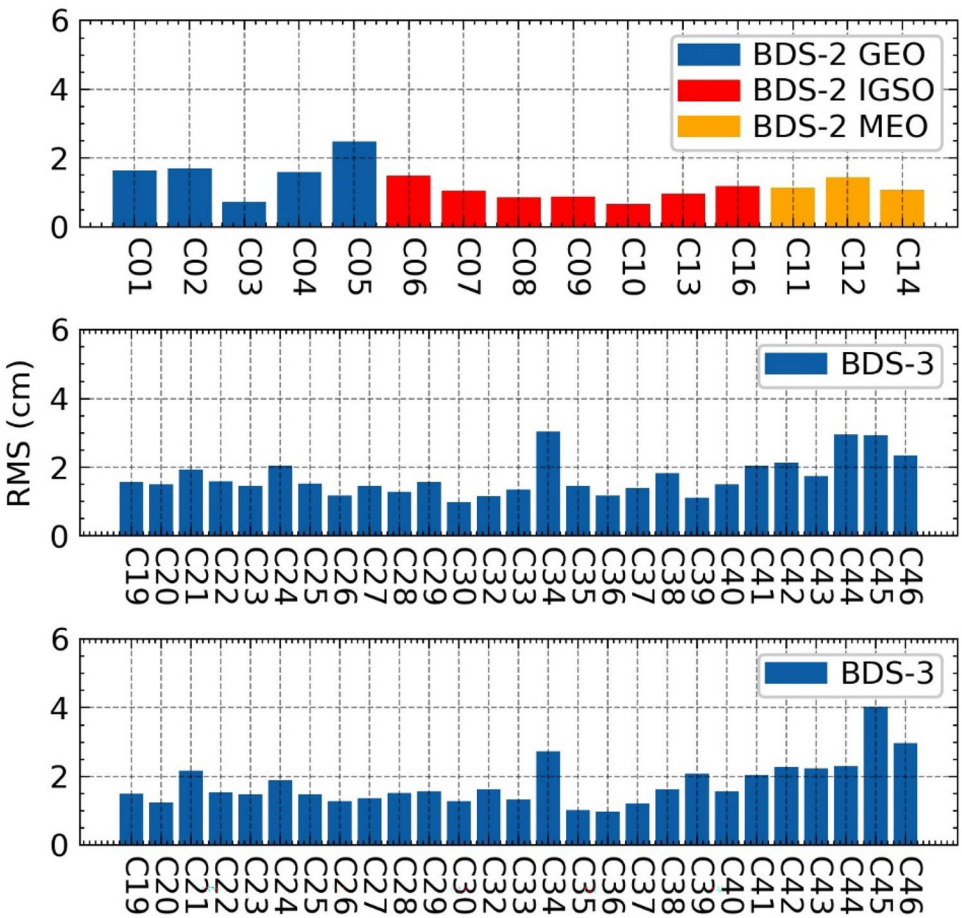

Fig. 8 RMS statistics of the estimated IFCBs for BDS-2 (top: B1I/B2I/B3I) and BDS-3 (middle: B1C/B2a/B3I; bottom: B1I/B2a/B3I) satellites

remained stable throughout the day. Moreover, Fig. 11 shows the STD statistics of the estimated EWL UPDs. The STDs of estimated EWL UPDs with IFCB corrections are significantly smaller than those with IFCB corrections, and the averaged STD of estimated EWL UPDs can be improved by 68.4% from 0.076 cycles to 0.024 cycles. Hence, the EWL UPDs of GPS satellites can be estimated daily with IFCB corrections rather than estimated epoch by epoch.

Figure 12 shows the positioning errors of GPS-only UC12-PPP and UC123-PPP solutions for two stations (BRST and HKSL). Here, we use 'UC12-PPP' and 'UC123-PPP' to represent the dual- and triple-frequency PPP float solutions with UC model, respectively. The green (UC123_NO) and yellow (UC123) dots in the figure represent the triple-frequency PPP float solutions without and with IFCB corrections, respectively, while the blue (UC12) dots in the figure indicate the results of dual-frequency PPP float solutions. It can be found that the positioning errors of UC123_NO solution exhibit observably larger variations than those of UC123 solution, especially on east and up components.

To further demonstrate the benefits of IFCB corrections on UC123-PPP, the statistics of average convergence time and positioning accuracy of 20 stations (shown in Fig. 13) from DOY 001 to DOY 007 of 2021 have been evaluated, and the results are presented in Table 2 and Fig. 14, respectively. Here, we defined the convergence time as the time needed to attain a horizontal positioning error less than 5 cm during 10 consecutive epochs (Feng and Wang 2008). Table 2 shows that the positioning accuracy of UC123-PPP solutions can be significantly improved by 30.3% from 4.56 to 3.18 cm, by 32.9% from 3.01 to 2.02 cm, and by 31.6% from 8.71 to 5.96 cm, in the east, north and up components, respectively, by using IFCB corrections. Meanwhile, from Fig. 14, the ratio of the convergence time less than 20 min has been improved from 67.5% to 70.8% by IFCB corrections. The average convergence

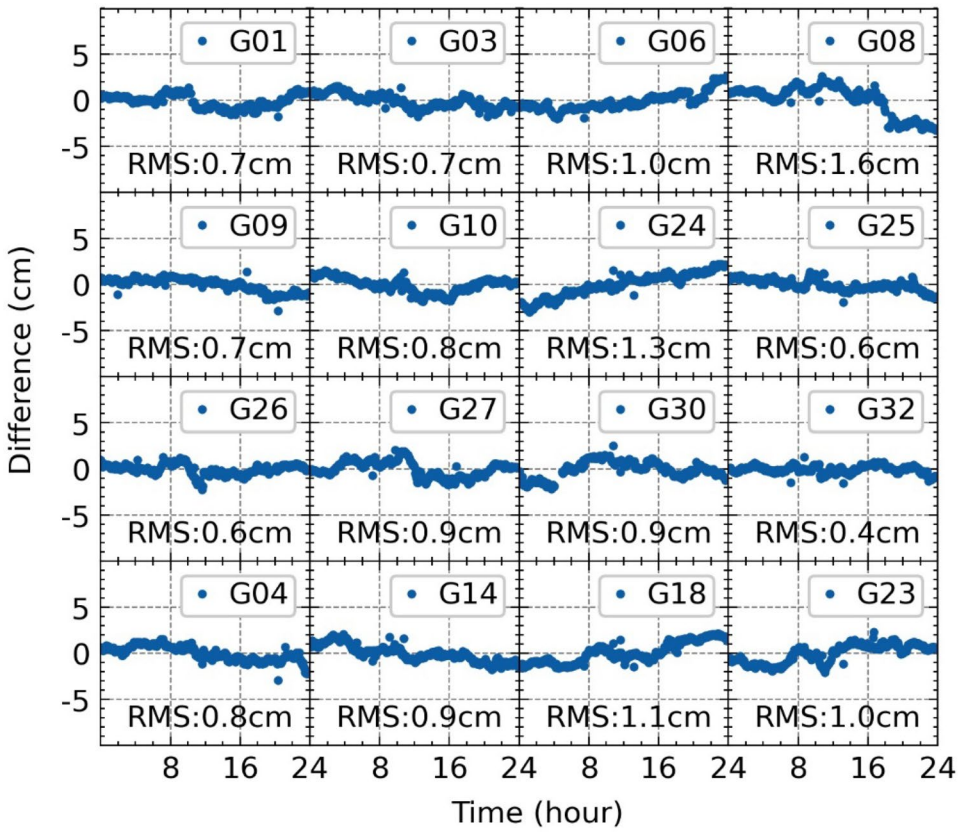

Fig. 9 Difference of IFCB estimation results based on GREAT-IFCB and PCE for GPS satellites on DOY 007 of 2021

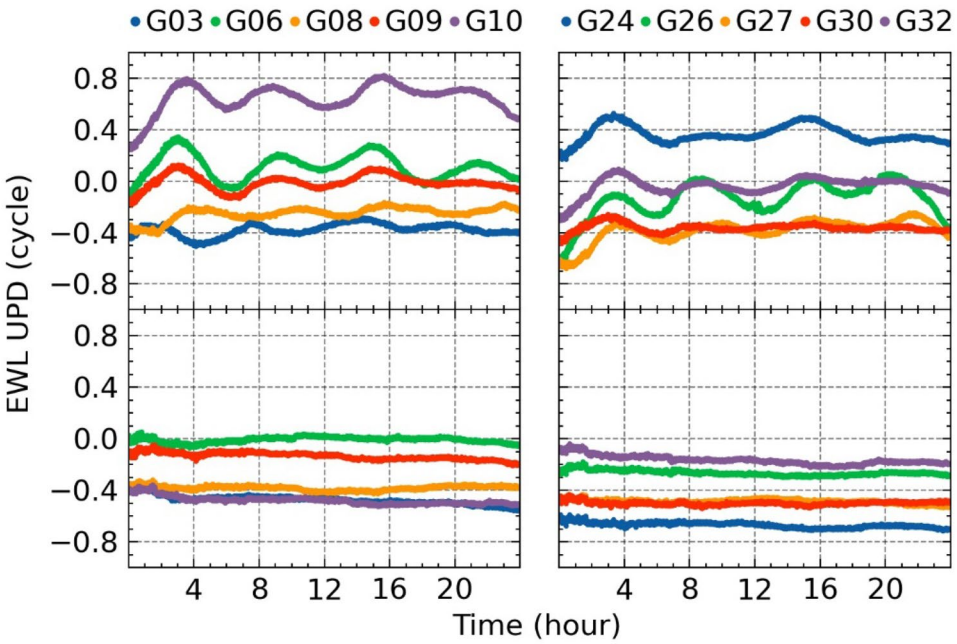

Fig. 10 Comparison of the estimated EWL UPDs of GPS satellites on DOY 001 of 2021 without (top) and with (bottom) IFCB corrections

time of UC123-PPP solutions is reduced by 17.2% from 21.08 to 17.45 min by using IFCB corrections, and it is marginally better than the 18.03 min of UC12-PPP solutions.

Conclusions

This study presents a software package for multi-GNSS IFCB estimation which is called GREAT-IFCB. The

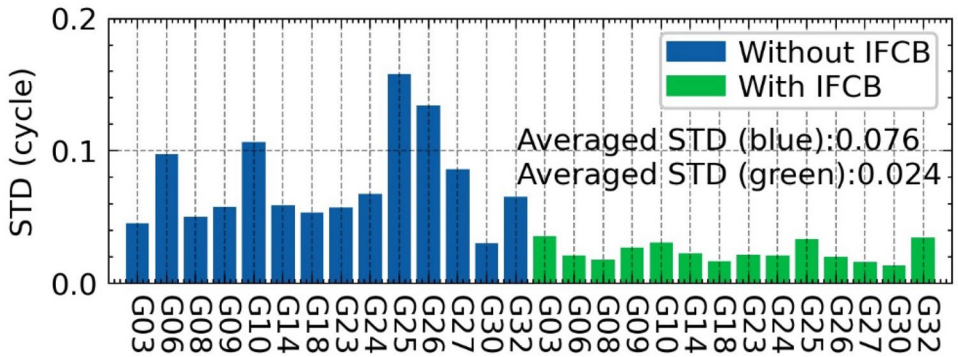

Fig. 11 STD statistics of estimated EWL UPDs for GPS without (blue) and with (green) IFCB corrections

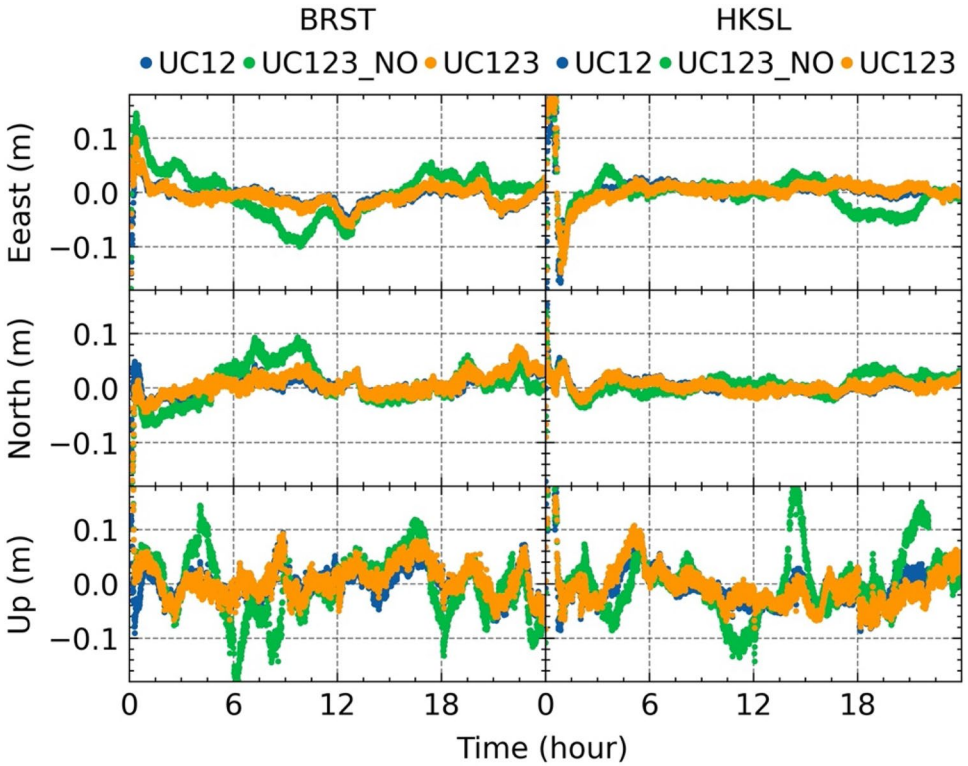

Fig. 12 Positioning errors of two stations BRST (left) and HKSL (right), which derived from GPS-only UC12-PPP solutions (blue) and UC123-PPP float solutions without (green) and with (yellow) IFCB corrections on DOY 001 of 2021

main structure of the software has been described in detail. Multi-frequency observations of 250 MGEX stations from DOY 001 to 007 of 2021 were used to estimate multi-GNSS IFCB products based on the GREAT-IFCB software. For GPS Block IIF satellites, the peak-to-peak amplitude of the estimated PIFCBs is about 10 cm, while the estimated PIFCBs of GPS III satellites and Galileo satellites exhibit a smaller variation of less than 2 cm. Meanwhile, the amplitude of the estimated PIFCBs for BDS satellites is smaller than 4 cm and the RMS values are smaller than 2 cm. Results indicate that GREAT-IFCB can generate available IFCB products for multi-GNSS satellites based on multi-frequency observations. Performance of the estimated EWL UPD and GPS-only UC123-PPP is also evaluated further to demonstrate the reliability of the estimated IFCB products. Based on the estimated

Table 2 Average positioning accuracy of GPS-only UC12- and UC123-PPP solutions without and with using IFCB corrections

	UC12	UC123_NO	UC123
East (cm)	3.22	4.56	3.18
North (cm)	2.02	3.01	2.02
Up (cm)	5.94	8.71	5.96

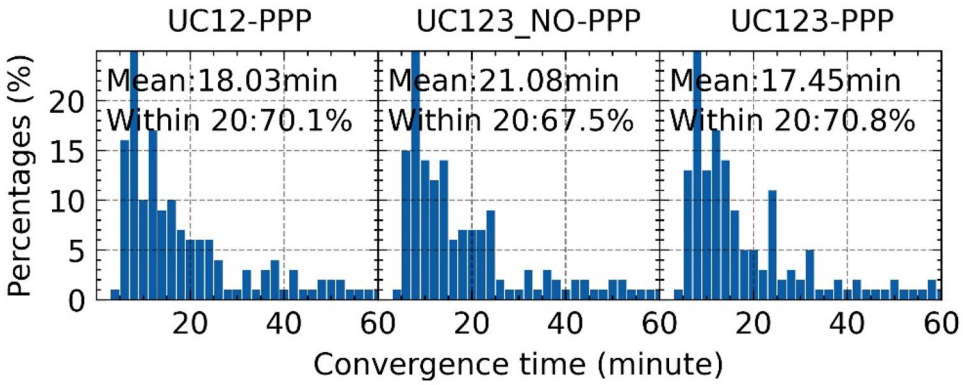

Fig. 14 Distribution of the convergence time of GPS-only UC12- and UC123-PPP solutions without and with IFCB corrections

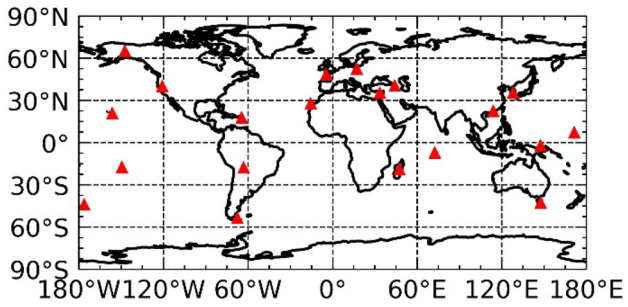

Fig. 13 Distribution of the stations used for PPP experiment

IFCB products, the STD of estimated EWL UPD for GPS satellites is improved by 68.4% from 0.076 cycles to 0.024 cycles, which means the EWL UPD can be estimated daily with IFCB corrections. As for the triple-frequency GPS-only PPP float solutions, the positioning accuracy of the solutions with IFCB corrections is 3.18, 2.02 and 5.96 cm in the east, north and up components, respectively, with the improvement of 30.3%, 32.9% and 31.6% compared to the solutions without IFCB corrections. Moreover, the average convergence time is reduced by 17.2% from 21.08 to 17.45 min by using IFCB corrections.

The source code of GREAT-IFCB and user manual are available at the website: https://geodesy.noaa.gov/gps-toolbox. GREAT-IFCB can be used to learn the fundamentals of GNSS and it can be extended for more features. GREAT-IFCB is a part of GREAT software platform, and more information about the GREAT platform is presented on the website: http://igmas.users.sgg.whu.edu.cn/software. The GREAT team welcomes comments and suggestions from readers and users, which will help to further improve the software platform.

Acknowledgements This work has been supported by the National Natural Science Foundation of China (Grant 41774030 and Grant 41974027), the frontier project of basic application from Wuhan science and technology bureau (Grant 2019010701011395), and the Sino-German mobility program (Grant No. M0054). The numerical calculations were done on the supercomputing system in the Supercomputing Center of Wuhan University.

References

Bock H, Dach R, Jäggi A, Beutler G (2009) High-rate GPS clock corrections from CODE: support of 1 Hz applications. J Geod 83:1083. https://doi.org/10.1007/s00190-009-0326-1

Cai C, He C, Santerre R, Pan L, Cui X, Zhu J (2016) A comparative analysis of measurement noise and multipath for four constellations: GPS, BeiDou, GLONASS and Galileo. Surv Rev 48(349):287–295. https://doi.org/10.1179/1752270615Y.0000000032

Deo M, El-Mowafy A (2018) Triple-frequency GNSS models for PPP with float ambiguity estimation: performance comparison using GPS. Surv Rev 50(360):249–261. https://doi.org/10.1080/00396265.2016.1263179

Fan L, Shi C, Li M, Wang C, Zheng F, Jing G, Zhang J (2019) GPS satellite inter-frequency clock bias estimation using triple-frequency raw observations. J Geod 93:2465–2479. https://doi.org/10.1007/s00190-019-01310-5

Feng Y, Wang J (2008) GPS RTK performance characteristics and analysis. J Glob Position Syst 7(1):1–8. https://doi.org/10.5081/jgps.7.1.1

Gao W, Gao C, Pan S, Wang D, Deng J (2015) Improving ambiguity resolution for medium baselines using combined GPS and BDS dual/triple-frequency observations. Sensors 15(11):27525–27542. https://doi.org/10.3390/s151127525

Ge M, Chen J, Douša J, Gendt G, Wickert J (2012) A computationally efficient approach for estimating high-rate satellite clock corrections in realtime. GPS Solut 16:9–17. https://doi.org/10.1007/s10291-011-0206-z

Geng J, Bock Y (2013) Triple-frequency GPS precise point positioning with rapid ambiguity resolution. J Geod 87:449–460. https://doi.org/10.1007/s00190-013-0619-2

Gu S, Lou Y, Shi C, Liu J (2015) BeiDou phase bias estimation and its application in precise point positioning with triple-frequency observable. J Geod 89:979–992. https://doi.org/10.1007/s00190-015-0827-z

Guo J, Geng J (2018) GPS satellite clock determination in case of inter-frequency clock biases for triple-frequency precise point positioning. J Geod 92:1133–1142. https://doi.org/10.1007/s00190-017-1106-y

Guo F, Zhang X, Wang J (2015) Timing group delay and differential code bias corrections for BeiDou positioning. J Geod 89:427–445. https://doi.org/10.1007/s00190-015-0788-2

Guo F, Zhang X, Wang J, Ren X (2016a) Modeling and assessment of triple-frequency BDS precise point positioning. J Geod 90:1223–1235. https://doi.org/10.1007/s00190-016-0920-y

Guo J, Xu X, Zhao Q, Liu J (2016b) Precise orbit determination for quad-constellation satellites at Wuhan University: strategy, result validation, and comparison. J Geod 90:143–159. https://doi.org/10.1007/s00190-015-0862-9

Hauschild A, Montenbruck O (2009) Kalman-filter-based GPS clock estimation for near real-time positioning. GPS Solut 13:173–182. https://doi.org/10.1007/s10291-008-0110-3

Li H, Zhou X, Wu B, Wang J (2012) Estimation of the inter-frequency clock bias for the satellites of PRN25 and PRN01. Sci China Phys Mech Astron 55:2186–2193. https://doi.org/10.1007/s11433-012-4897-0

Li P, Zhang X, Ge M, Schuh H (2018) Three-frequency BDS precise point positioning ambiguity resolution based on raw observables. J Geod 92:1357–1369. https://doi.org/10.1007/s00190-018-1125-3

Li X, Li X, Liu G, Feng G, Yuan Y, Zhang K, Ren X (2019) Triple-frequency PPP ambiguity resolution with multi-constellation GNSS: BDS and Galileo. J Geod 93:1105–1122. https://doi.org/10.1007/s00190-019-01229-x

Li X, Liu G, Li X, Zhou F, Feng G, Yuan Y, Zhang K (2020) Galileo PPP rapid ambiguity resolution with five-frequency observations. GPS Solut 24:24. https://doi.org/10.1007/s10291-019-0930-3

Li X, Han X, Li X, Liu G, Feng G, Wang B, Zheng H (2021a) GREAT-UPD: An open-source software for uncalibrated phase delay estimation based on multi-GNSS and multi-frequency observations. GPS Solut 25:66. https://doi.org/10.1007/s10291-020-01070-2

Li X, Huang J, Li X, Lyu H, Wang B, Xiong Y, Xie W (2021b) Multi-constellation GNSS PPP instantaneous ambiguity resolution with precise atmospheric corrections augmentation. GPS Solut 25:107. https://doi.org/10.1007/s10291-021-01123-0

Liu G, Zhang X, Li P (2019) Improving the performance of Galileo uncombined precise point positioning ambiguity resolution using triple-frequency observations. Remote Sensing 11(3):341. https://doi.org/10.3390/rs11030341

Malys S, Jensen PA (1990) Geodetic point positioning with GPS carrier beat phase data from the CASA UNO experiment. Geophys Res Lett 17(5):651–654. https://doi.org/10.1029/GL017i005p00651

Montenbruck O, Hugentobler U, Dach R et al (2012) Apparent clock variations of the block IIF-1 (SVN62) GPS satellite. GPS Solut 16:303–313. https://doi.org/10.1007/s10291-011-0232-x

Montenbruck O, Hauschild A, Steigenberger P, Hugentobler U,Teunissen P, Nakamura S (2013) Initial assessment of theCOMPASS/BeiDou-2 regional navigation satellite system. GPSSolut 17(2):211–222. https://doi.org/10.1007/s10291-012-0272-x

Montenbruck O, Steigenberger P, Prange L, Deng Z, Zhao Q, Perosanz F, Romero I, Noll C, Stürze A, Weber G, Schmid R, MacLeod K, Schaer S (2017) The multi-GNSS experiment (MGEX) of the international GNSS service (IGS)—achievements, prospects and challenges. Adv Space Res 59(7):1671–1697. https://doi.org/10.1016/j.asr.2017.01.011

Moreno Monge B, Rodríguez-Caderot G, de Lacy M (2014) Multi-frequency algorithms for precise point positioning: MAP3. GPS Solut 18:355–364. https://doi.org/10.1007/s10291-013-0335-7

Pan L, Li X, Zhang X, Li X, Lu C, Zhao Q, Liu J (2017) Considering inter-frequency clock bias for BDS triple-frequency precise point positioning. Remote Sens 9(7):734. https://doi.org/10.3390/rs9070734

Pan L, Zhang X, Guo F, Liu J (2019) GPS inter-frequency clock bias estimation for both uncombined and ionospheric-free combined triple-frequency precise point positioning. J Geod 93:473–487. https://doi.org/10.1007/s00190-018-1176-5

Thoelert S, Steigenberger P, Montenbruck O, Meurer M (2019) Signal analysis of the first GPS III satellite. GPS Solut 23:92. https://doi.org/10.1007/s10291-019-0882-7

Vaclavovic P, Dousa J, Gyori G (2013) G-Nut software library - state of development and first results. Acta Geodyn Geomater 10(4):431–436. https://doi.org/10.13168/AGG.2013.0042

Wang K, Khodabandeh A, Teunissen P (2018) Five-frequency Galileo long-baseline ambiguity resolution with multipath mitigation. GPS Solut 22:75. https://doi.org/10.1007/s10291-018-0738-6

Zhao Q, Wang G, Liu Z, Hu Z, Dai Z, Liu J (2016) Analysis of BeiDou satellite measurements with code multipath and geometry-free ionospheric-free combinations. Sensors 16(1):123. https://doi.org/10.3390/s16010123

Zhao L, Ye S, Chen D (2019) Numerical investigation on the effects of third-frequency observable on the network clock estimation model. Adv Space Res 63(9):2930–2937. https://doi.org/10.1016/j.asr.2018.03.004

Zumberge J, Heflin M, Jefferson D, Watkins M, Webb F (1997) Precise point positioning for the efficient and robust analysis of GPS data from large networks. J Geophys Res 102(B3):5005–5017. https://doi.org/10.1029/96JB03860

Xingxing Li has completed his B.Sc. degree at the School of Geodesy and Geomatics in Wuhan University and obtained his Ph.D. degree at the Department of Geodesy and Remote Sensing of the German Research Centre for Geosciences (GFZ). He is currently a professor at Wuhan University. His current research mainly involves GNSS precise data processing and its application for geosciences.

Hongjie Zheng is currently a Ph.D. candidate at Wuhan University. He has completed his B.Sc. and Master's degree at the School of Geodesy and Geomatics in Wuhan University in 2019 and 2022. His area of research currently focuses on multi-GNSS precise orbit determination.

Xin Li is currently a Postdoc at Wuhan University. She received a B.Sc. and Ph.D. degree at the School of Geodesy and Geomatics at Wuhan University in 2015 and 2021. Her area of research currently focuses on multi-GNSS PPP ambiguity resolution.

Yongqiang Yuan is currently a Postdoc at Wuhan University. He has completed his Ph.D. degree at the School of Geodesy and Geomatics in Wuhan University in 2022. His area of research currently focuses on GNSS precise orbit determination and the geodetic parameter estimation with GNSS satellites.

Jiaqi Wu is currently a Ph.D. candidate at Wuhan University. He has completed his B.Sc. at the School of Geodesy and Geomatics at Wuhan University in 2019. His area of research currently focuses on multi-GNSS precise orbit determination.

Xinjuan Han is currently a Master′s candidate at Wuhan University. She has completed her B.Sc. at the School of Geodesy and Geomatics at Wuhan University in 2019. Her area of research currently focuses on multi-GNSS PPP ambiguity resolution.